Electrochemical study and analytical applications for new biologically active 2-nitrophenylbenzimidazole derivatives

A. Álvarez-Lueje*, C. Zapata-Urzúa, S. Brain-Isasi, M. Pérez-Ortiz, L. Barros, H. Pessoa-Mahana, M.J. Kogan

Bioelectrochemistry Laboratory, Chemical and Pharmaceutical Sciences Faculty, University of Chile, P.O. Box 233, Santiago 1, Chile

ABSTRACT

The present study addresses the electrochemical behavior and the analytical applications of six 2-nitrophenylbenzimidazole derivatives with activity against *Trypanosoma cruzi*. When studied in a wide range of pH, by differential pulse polarography, tast polarography and cyclic voltammetry, these compounds exhibited two irreversible cathodic responses. With analytical purposes, the differential pulse polarography mode was selected, which exhibited adequate analytical parameters of repeatability, reproducibility and selectivity. The percentage of recovery was in all cases over 99%, and the detection and quantitation limits were at the level of 1×10^{-7} mol L^{-1} and 1×10^{-6} mol L^{-1}, respectively. In addition, the differential pulse polarography method was successfully applied to study the hydrolytic degradation kinetic of one of the tested compounds. Activation energy, kinetic rate constants at different temperatures and half-life values of such application are reported.

Keywords:
2-Nitrophenylbenzimidazole
Differential pulse polarography
Tast polarography
Cyclic voltammetry

1. Introduction

Parasitic diseases are a public health problem in many countries of the world. It is reported that approximately 18 million of people are infected with *Trypanosoma cruzi*, the protozoa responsible of Chagas' disease, especially in rural and poor areas in South and Latin America [1]. At present, there are two available drugs for the treatment of Chagas' disease: nifurtimox and benznidazole, which have significant activity in the acute phase of the disease, although limited efficacy in the chronic stages, carrying severe side effects [2].

Compounds with benzimidazolic nucleus present a wide spectrum of biological activities such as antiparasitic, antibacterial, antiviral and antitumoral, amongst others [3,4].

On the other hand, nitroaromatic compounds have proven antiparasitic, antibacterial, antimycotic and antitumoral activities, which are related to their electrochemical properties. The nitro group is very reactive in the presence of oxygen, and its complete reduction involves the addition of 6 electrons to form the amine, *via* nitro radical anion ($1e^-$), nitroso ($2e^-$) and hydroxylamine ($4e^-$) intermediates [5–8].

There is evidence that free-radical metabolites from nitroaromatics compounds can cause deleterious effects in bacteria, parasitic and mammalian cells, which can be correlated with the pharmacological activity of these compounds. According to the $E_{1/2}$ values determined in aqueous solutions by cyclic voltammetry or polarography, the reduction of the nitro group is not reversible and may involve the addition of up to 4 electrons, being the first one usually the most difficult to add [9].

According to the above, combining a benzimidazole nucleus with a nitroaromatic ring could result in compounds with relevant biological activity against parasites. In a previous report [10], using HPLC and UV-spectrophotometric techniques we characterized a new series of 2-nitrophenylbenzimidazole derivatives which exhibited growth and oxygen uptake inhibitory effects in *T. cruzi* epimastigotes. Aiming to further studying these compounds and taking into account the relevance of the electrochemical properties on their biological activity, in this work we have addressed the electrochemical behavior and the development of electroanalytical methods for the following six nitrophenylbenzimidazole derivatives: 2-(2-nitrophenyl)-1H-benzimidazole (NB), 1-benzoyl-2-(2-nitrophenyl)-benzimidazole (BNB), 1-(4-methoxybenzoyl)-2-(2-nitrophenyl)-benzimidazole (PMNB), 1-(4-chlorobenzoyl)-2-(2-nitrophenyl)-benzimidazole (PCNB), 1-(4-fluorobenzoyl)-2-(2-nitrophenyl)-benzimidazole (PFNB) and 1-(4-nitrobenzoyl)-2-(2-nitrophenyl)-benzimidazole (PNB) (Fig. 1).

2. Experimental

2.1. Reagents and drugs

2-(2-Nitrophenyl)-1H-benzimidazole ($C_{13}H_9N_3O_2$, MW: 239.06 g mol^{-1}, MP: 277–278.5 °C); 1-benzoyl-2-(2-nitrophenyl)-

* Corresponding author. Fax: +56 7378920.
E-mail address: aalvarez@ciq.uchile.cl (A. Álvarez-Lueje).

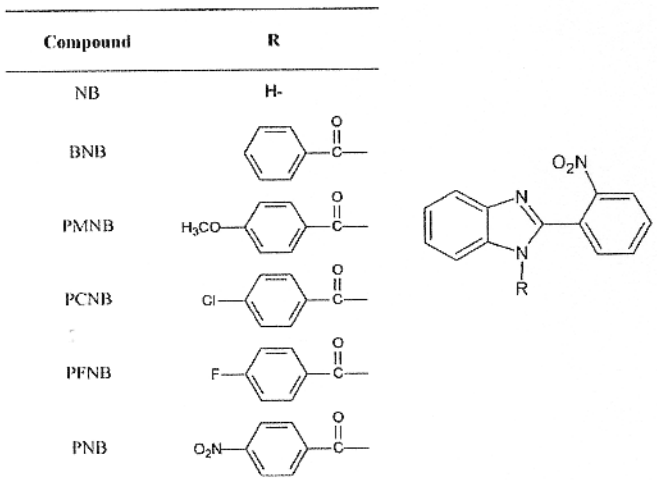

Fig. 1. Chemical structures of 2-(2-nitrophenyl)-1H-benzimidazole (NB), 1-benzoyl-2-(2-nitrophenyl)-1H-benzimidazole (BNB), 1-(4-methoxybenzoyl)-2-(2-nitrophenyl)-1H-benzimidazole (PMNB), 1-(4-chlorobenzoyl)-2-(2-nitrophenyl)-1H-benzimidazole (PCNB), 1-(4-fluorobenzoyl)-2-(2-nitrophenyl)-benzimidazole (PFNB) and 1-(4-nitrobenzoyl)-2-(2-nitrophenyl)-1H-benzimidazole (PNB).

benzimidazole ($C_{20}H_{13}N_3O_3$, MW: 343.33 g mol^{-1}, MP: 161 °C); 1-(4-methoxybenzoyl)-2-(2-nitrophenyl)-benzimidazole ($C_{21}H_{15}N_3O_4$, MW: 373.36 g mol^{-1}, MP: 124–126 °C); 1-(4-chlorobenzoyl)-2-(2-nitrophenyl)-benzimidazole ($C_{20}H_{12}N_3O_3Cl$, MW: 377.78 g mol^{-1}, MP: 127–129 °C); 1-(4-fluorobenzoyl)-2-(2-nitrophenyl)-benzimidazole ($C_{20}H_{12}N_3O_3F$, MW: 361.33 g mol^{-1}, MP: 165–166 °C) and 1-(4-nitrobenzoyl)-2-(2-nitrophenyl)-benzimidazole ($C_{20}H_{12}N_4O_5$, MW: 388.33 g mol^{-1}, MP: 174–176.9 °C) were obtained in our laboratory according to a procedure previously described [11,12]. The purity of these compounds was assessed by ^{1}H NMR, ^{13}C NMR, IR and melting point. All reagents were of analytical grade, unless indicated otherwise. Methanol and acetonitrile, HPLC grade, were used. Deionized water was obtained in the laboratory, using ionic exchange columns (Milli-Q).

2.2. Solutions preparation

2.2.1. Buffer solutions

0.1 mol L^{-1} Britton–Robinson buffer (acetic acid/boric acid/phosphoric acid) [13] was used for polarographic experiments, and desired pH adjusted with NaOH or HCl concentrated solutions.

2.2.2. Stock drug solutions

NB and BNB were dissolved in ethanol. PMNB, PCNB, PFNB and PNB were dissolved in acetonitrile. All solutions were prepared to a final concentration of 1×10^{-3} mol L^{-1}, and protected from light using amber glass material.

2.2.3. Work solutions

For differential pulse polarographic (DPP) and tast polarographic (TP) experiments in protic medium, 2.5 mL aliquots of the NB and BNB stock solutions were taken and then diluted to 25 mL with ethanol/0.1 mol L^{-1} Britton–Robinson buffer solution (final ratio of 30/70 v/v). For the other compounds 2.5 mL aliquots were taken and diluted to 25 mL with acetonitrile/0.1 mol L^{-1} Britton–Robinson buffer solution (final ratio of 30/70 v/v for PFNB and 50/50 v/v for PMNB and PCNB) or acetonitrile/0.2 mol L^{-1} phosphate buffer solution for PNB (final ratio of 50/50 v/v).

For cyclic voltammetric (CV) experiments in protic medium, working solutions were employed as previously described. In non-aqueous medium, the studies were carried out in dimethylformamide containing as supporting electrolyte tetrabutylammonium perchlorate (0.1 mol L^{-1}). All the compounds were employed at 1×10^{-3} mol L^{-1} concentration.

2.3. Apparatus

2.3.1. Voltammetric analyzer

DPP and TP experiments were performed with a Metrohm Model 693 VA-Processor, equipped with a model 694 VA-stand. A 25-mL thermostated Metrohm measuring cell, equipped with either a dropping or a hanging mercury electrode (Metrohm) as the working electrode, a platinum wire counter electrode and a calomel reference electrode, was employed. The operating conditions were: sensitivity 2.5–10 μA; drop time 0.6 s; potential range 0 to −1800 mV; ΔE_p −6 mV; pulse retard 40 ms; pulse height −50 mV. CV experiments were performed in a Bioanalytical System (BAS), CV-50W, couple to Pentium computer with CV-50W acquisition and treatment program.

2.4. Molecular modeling

All calculations were run on a SGI workstation and the protocol for the iterative simulated annealing (ISA) calculations was similar to one previously described [14]. This protocol was run five times, employing fully extended starting structures of NB, BNB, PMNB, PCNB, PFNB and PNB, obtaining the same global minimums each time for each compound.

2.5. Analytical procedure

2.5.1. Calibration curve preparation

Working solutions, ranging between 1×10^{-6} mol L^{-1} and 1×10^{-4} mol L^{-1}, were prepared by diluting each stock solution with ethanol/0.1 mol L^{-1} Britton–Robinson buffer pH 4.0 for NB, pH 5.0 for BNB (final ratio of 30/70 v/v) or acetonitrile/0.1 mol L^{-1} Britton–Robinson buffer pH 6 for PMNB and PCNB (final ratio of 50/50 v/v), pH 7 for PFNB (final ratio of 30/70 v/v) or acetonitrile/0.2 mol L^{-1} phosphate buffer pH 7 for PNB (final ratio of 50/50 v/v).

2.5.2. Selectivity studies [15]

2.5.2.1. Degradation trials. Hydrolysis: 1 mL of each compound stock solution was placed in a 10 mL-distillation flask and (a) 5 mL 0.1 mol L^{-1} HCl for acid hydrolysis or (b) 5 mL 0.1 mol L^{-1} NaOH for basic hydrolysis, was added. Then each solution was boiled for 3 h at reflux.

Photolysis: Separately, 3 mL of each compound stock solution were placed in UV-cells and disposed on a black box and then irradiated with UV light (UV black-ray long wave UV lamp, UVP model B 100 AP, 50 Hz, 2.0 A, with a 100 W Par 38 Mercury lamp equipped with a 366 nm filter) at a distance of 15 cm for 8 h (1.2×10^{19} quanta s^{-1}, determined by using potassium ferrioxalate chemical actinometer [16]).

Samples of each of the solutions obtained through the degradation trials were diluted, as previously described in Section 2.2.3, with ethanol/0.1 mol L^{-1} Britton–Robinson buffer, acetonitrile/0.1 mol L^{-1} Britton–Robinson buffer or with acetonitrile/0.2 mol L^{-1} phosphate buffer, to obtain a theoretical concentration of 5×10^{-5} mol L^{-1}. Each sample was analyzed in duplicate.

2.5.2.2. Pharmaceutical interferents. Typical pharmaceutical excipients: cornstarch, magnesium stearate, lactose, sodium lauryl sulfate, titanium dioxide, sodium carbonate, polyethylenglycol 400 and 4000, hydroxypropylcellulose, hydroxypropylmethylcelullose, sorbitol, talc, sodium starch glycolate/sodium carboxymethyl starch (Explotab®) and microcristalline cellulose (Avicel® pH 101), were tested.

2.5.2.3. Stability studies. A stock solution of BNB was diluted to obtain an initial concentration ranging between 1.0×10^{-4} mol L^{-1} and 1.0×10^{-5} mol L^{-1} in a final ratio of 30/70 (v/v) ethanol/0.1 mol L^{-1} Britton–Robinson buffer solution, at selected pH (3, 4, 5, 6, 7.4, 8, 9 and 10), and its degradation was studied at 25 °C. The solution prepared at pH 7.4 was further studied by placing in an oven at 25 °C, 40 °C and 60 °C (±0.2 °C) samples contained in 2 mL amber vials (at least two for each point of the degradation curve). According to the temperature of exposure, vials were removed from the oven at selected time intervals (at 30 min, 20 min and 10 min for 25 °C, 40 °C and 60 °C, respectively), placed on ice immediately after to quench the reaction, and assayed by DPP. Degradation experiments were carried out in duplicate and monitored, at least, over three half-lives.

2.5.2.4. Activation energy (E_a). Each E_a value was obtained from Arrhenius model, by plotting $\ln k$ *vs.* $1/T$ for each concentration tested. The final E_a value represents the average of the E_a calculated for a concentration of 1×10^{-4} mol L^{-1} at pH 7.4. In all cases, regression coefficient values higher than 0.993 were obtained.

3. Results and discussion

3.1. Electrochemical studies

NB, BNB, PMNB, PCNB and PFNB in protic media were reduced on a mercury electrode surface. The polarograms obtained by DPP or TP exhibit, in a broad range of pH, two peaks or two waves, respectively. In all cases, the main signal obtained (I) is a well-resolved peak. The second signal appears at more negative potentials and lower peak

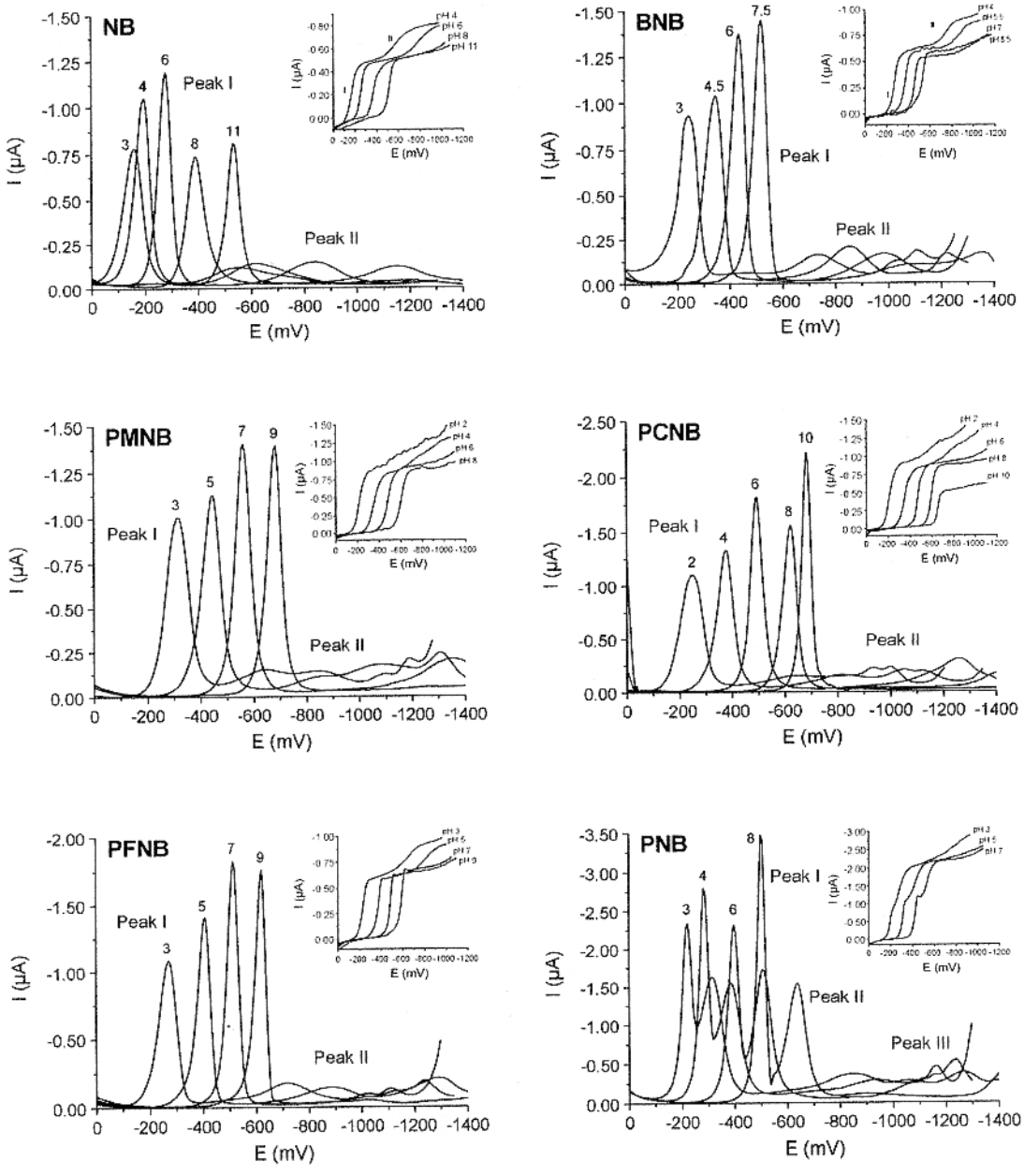

Fig. 2. DPP evolution with pH of 2-nitrophenylbenzimidazole derivatives. Insert: TP dependence with pH.

currents (II). Fig. 2 depicts the polarographic evolution of the compounds as a function of the pH. At low potentials, the first signal (I) for these compounds would correspond to the reduction of the nitro group, generating the hydroxylamine derivative, which involves 4-electrons, according to [17]: $R\text{-}NO_2 + 4e^- + 4H^+ \rightarrow R\text{-}NHOH + H_2O$. On the other hand, signal II is likely to correspond to the azomethine reduction [18–20].

Unlike the above, PNB exhibits a more complex polarogram with two overlapped signals, due to the presence of two nitro groups in its structure. Regardless of the organic solvent/buffer solution used (acetonitrile/Britton–Robinson, methanol/phosphate, dimethylformamide/phosphate, acetonitrile/phosphate); these signals could not be well resolved. By comparing the polarographic responses of the other N-substituted derivatives studied with PNB, signal I would correspond to the p-nitro reduction, signal II to the o-nitro reduction and signal III to the azomethine reduction.

Peak potential evolution with pH is shown in Fig. 3. As can be seen, peaks potential I and II shift towards more cathodic potential as the pH increases, exhibiting a linear dependence with pH, reaching a pH-independent behavior from pH 9–12 (peak II) for NB. Also, for the main peak (I), breaks in the linear response are clearly observed for NB, BNB and PFNB, between pH 4 and 5; probably due to the pK_a values of these derivatives. In the TP mode, all studied compounds presented dependence between $E_{1/2}$ and the pH, showing breaks at around pH 5. Table 1 summarizes the slopes of the linear segments and the corresponding breaks for each of the studied compound. As can be seen, the amphoteric compound NB exhibits a lower dependence with the pH for the first signal ($\delta E_{1/2}/\delta pH \sim 30\,mV\,pH^{-1}$). Such behavior differs from that of the other N-substituted derivatives, which are weak bases and exhibit slopes around twice greater ($\delta E_{1/2}/\delta pH$ between $65\,mV\,pH^{-1}$ and $71\,mV\,pH^{-1}$); these structural and acid–base differences between NB and the others compounds would produce changes in the electrodic mechanism, affecting the α_n term (where α is the transfer coefficient) that translates into a significant change in the slope of the potential *vs.* pH plot [21]. In a previous report, we calculated the

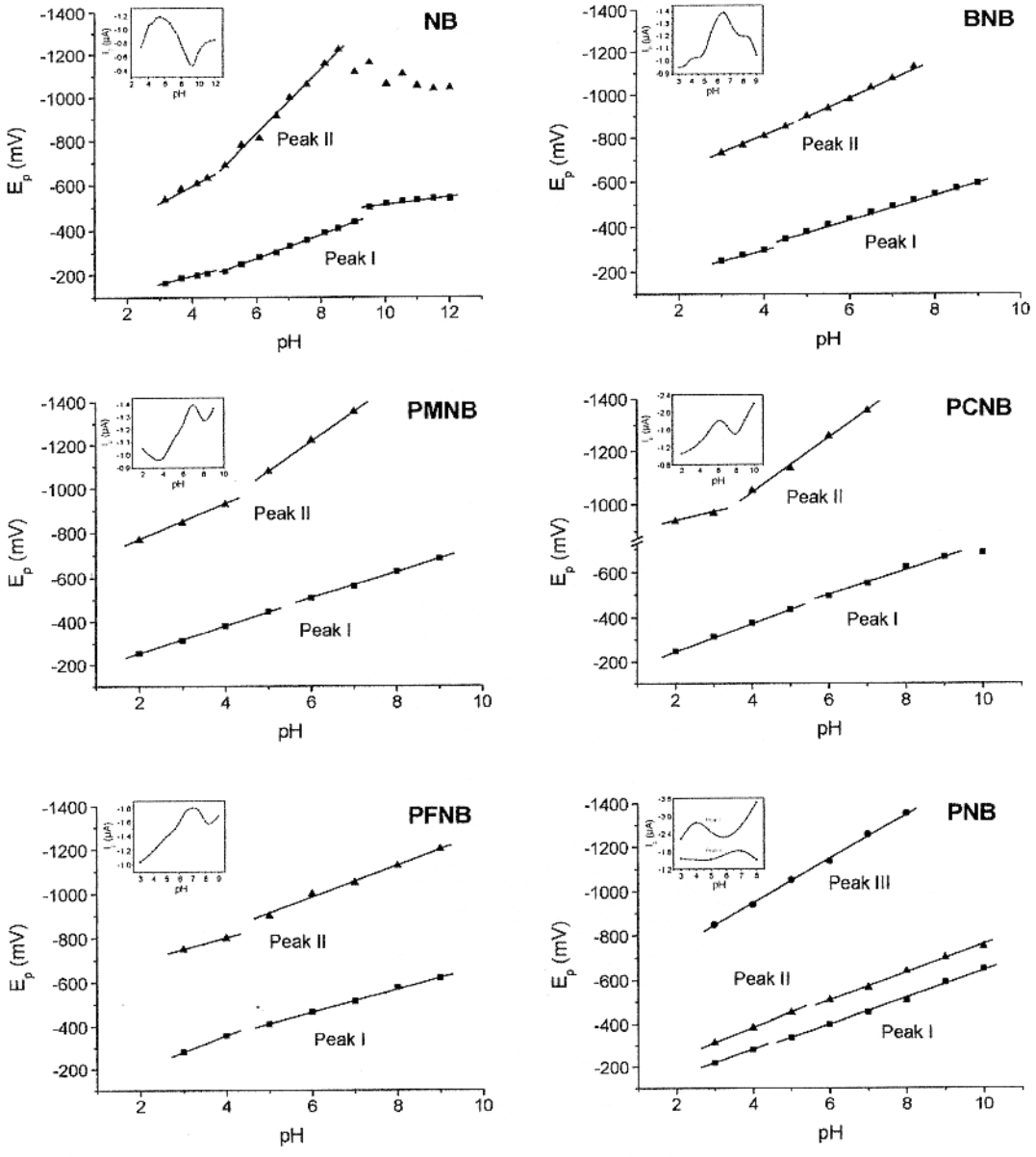

Fig. 3. Peak potential evolution with pH of 2-nitrophenylbenzimidazole derivatives. Insert: peak current dependence with pH.

Table 1
$\delta E_{1/2}/\delta$pH values for the linear segments for the 2-nitrophenylbenzimidazole derivatives in protic media (signal I, TP).

Compound	1st segment, mV pH^{-1} (pH range)	2nd segment, mV pH^{-1} (pH range)
NB	29.6 (2–4.5)	52.6 (4.5–9.5)
BNB	69.7 (2–5.5)	55.3 (5.5–9)
PMNB	65.7 (2–6)	59.1 (6–9)
PCNB	65.6 (2–6)	55.7 (6–9)
PFNB	71 (2–5.5)	51.1 (5.5–9)
PNB	58.5 (2–5)[a]; 69.6 (2–5)[b]	55.6 (5–8)[a]; 61.9 (5–8)[b]

[a] Signal I.
[b] Signal II.

pK_a value of each compound by means of UV-spectrophotometry [10]; NB exhibits two pK_a values, 5.69 and 11.38 for the N=C and NH, respectively, unlike other benzimidazole derivatives that present only one pK_a value, corresponding to their weak base imidazole nitrogen ($pK_{a\,BNB} = 4.90$; $pK_{a\,PMNB} = 4.71$; $pK_{a\,PCNB} = 4.69$; $pK_{a\,PFNB} = 4.86$ and $pK_{a\,PNB} = 4.79$). These values are in agreement with the breaks observed above in the electrochemical studies. On the other hand, it can be seen that the peak current reaches its maximum value near pH 6 and its behavior is consistent with peak potential evolution seen for peak I (insert in Fig. 3).

The differences in the reduction potentials seen between the various 2-nitrophenylbenzimidazole derivatives could be explained by either, the loss of coplanarity of the nitro group from the plane with respect to the phenyl ring, as a consequence of a steric effect of the 2-benzimidazole substituent [22], or the staking of the phenyl ring of the 2-nitrophenylbenzimidazole nucleus with that of the N-benzoyl substituent. In either case, a reduction of the nitro group at the electrode would become more difficult to occur [23]. Thus, the distortion of the coplanar arrangement diminishes the resonance between the nitro group and the aromatic system, producing shifts towards more negative potentials. These effects can be clearly appreciated when the peak potentials of NB (without N-substitution) and BNB (N-benzoyl substituted) are compared with that of the others N-p-benzoyl substituted derivatives; while the former exhibit values of −360 mV and −490 mV, the latter present peak potentials higher than −500 mV (values obtained in acetonitrile/0.1 mol L^{-1} Britton–Robinson buffer, 30/70 v/v, pH 7). In order to support the above assumptions, a conformational search to find the global minimum conformers for each compound was carried out using an ISA calculation [14]. Unlike the other compounds, NB shows no coplanarity or staking phenomena (due to the absence of a N-benzoyl substituent) (Fig. 4A). In the case of BNB, the staking was partial (Fig. 4B) while for the other compounds such effect was complete, shifting the potential to more negative values (Fig. 4C depicts the case of PFNB).

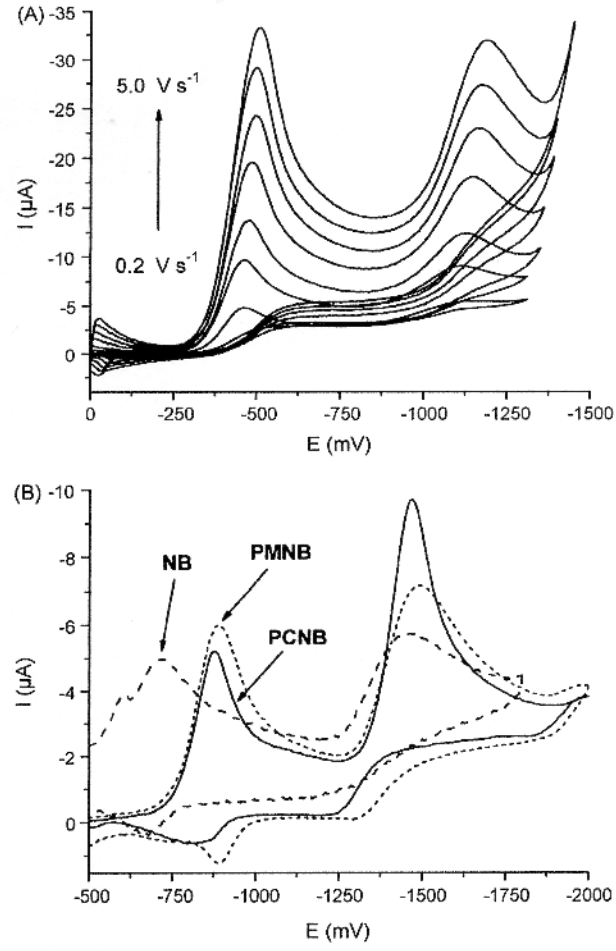

Fig. 5. Cyclic voltammograms of (A) 1×10^{-3} mol L^{-1} PCNB in acetonitrile/0.1 mol L^{-1} Britton–Robinson buffer (50/50 v/v) at different sweep rates; (B) 1×10^{-3} mol L^{-1} solutions of NB, PMNB and PCNB in non-aqueous medium at 1 V s^{-1}.

Additionally, CV studies were conducted at different pH and sweep rates (Fig. 5A). In protic media, the 2-nitrophenylbenzimidazole derivatives displayed, at all pH (3, 7 and 10) and scan rate (0.1–10 V s^{-1}) studied, an irreversible signal, being observed that each signal moves towards more negative potentials as the pH was increased (data not shown).

Upon analyzing the relationship between peak current and sweep rate ($\log I_p$ *vs.* log sweep rate plot), slope values near to

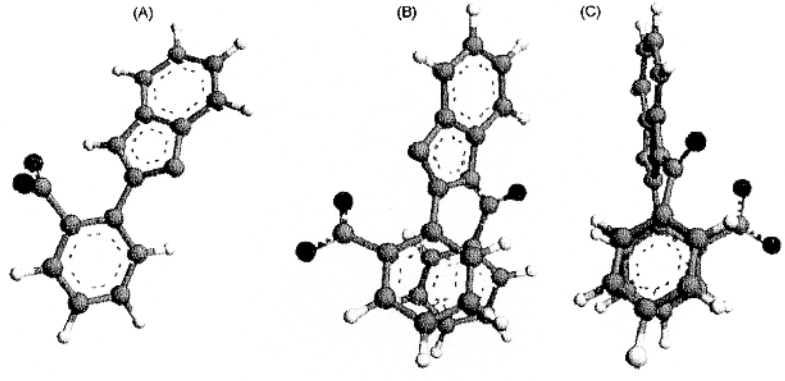

Fig. 4. Ball and Stick conformational representation of global minimum energy conformer of NB (A), BNB (B) and PFNB (C).

Table 2
Analytical parameters of 2-nitrophenylbenzimidazole derivatives by DPP.

	NB[a]	BNB[b]	PMNB[c]	PCNB[c]	PFNB[d]	PNB[e]
Potential detection (mV)	−119	−373	−500	−494	−519	−652
Repeatability, CV (%) 3×10^{-6} mol L^{-1}; 1×10^{-5} mol L^{-1}; 7×10^{-5} mol L^{-1}	1.0; 0.4; 1.7	2.4; 2.2; 0.6	1.2; 1.3; 1.4	1.0; 1.8; 1.6	1.7; 0.9; 0.4	0.59; 0.59; 1.3
Reproducibility, CV (%) 3×10^{-6} mol L^{-1}; 1×10^{-5} mol L^{-1}; 7×10^{-5} mol L^{-1}	1.5; 2.6; 2.3	1.4; 1.5; 1.4	1.8; 1.4; 1.4	1.36; 1.74; 1.77	1.4; 1.2; 1.1	0.49; 0.67; 1.8
Recovery (%) ±s.d.	99.0 ± 0.6	99.1 ± 0.8	102.6 ± 1.4	102.5 ± 2.7	99.3 ± 0.5	99.1 ± 0.8
Concentration range (mol L^{-1})	1×10^{-6}–7×10^{-5}	1×10^{-6}–7×10^{-5}	4×10^{-6}–3×10^{-5}	4×10^{-6}–1×10^{-5}	4×10^{-6}–2×10^{-5}	4×10^{-6}–5×10^{-5}
Calibration curve (i_p, nA; [c], mol L^{-1})	$i_p = 1.28\times10^{7}$ [c] + 4.29 (r = 0.9977, n = 8)	$i_p = 1.0\times10^{7}$ [c] + 4.39 (r = 0.9999, n = 7)	$i_p = 1.5\times10^{7}$ [c] − 1.9 (r = 0.9999, n = 7)	$i_p = 1.8\times10^{7}$ [c] + 4.9 (r = 0.9995, n = 7)	$i_p = 1.58\times10^{7}$ [c] + 14.1 (r = 0.9998, n = 6)	$i_p = 1.63\times10^{7}$ [c] + 5.1 (r = 0.9998, n = 6)
Detection limit (mol L^{-1})	4.5×10^{-7}	7.8×10^{-7}	7.5×10^{-7}	5.9×10^{-7}	2.8×10^{-6}	5.4×10^{-6}
Quantitation limit (mol L^{-1})	1.2×10^{-6}	2.5×10^{-6}	1.6×10^{-7}	1.4×10^{-6}	6.5×10^{-6}	1.7×10^{-5}

[a] Ethanol/0.1 mol L^{-1} Britton–Robinson buffer (30/70 v/v) pH 4.
[b] Ethanol/0.1 mol L^{-1} Britton–Robinson buffer (30/70 v/v) pH 5.
[c] Acetonitrile/0.1 mol L^{-1} Britton–Robinson buffer (50/50 v/v) pH 6.
[d] Acetonitrile/0.1 mol L^{-1} Britton–Robinson buffer (30/70 v/v) pH 7.
[e] Acetonitrile/0.2 mol L^{-1} phosphate buffer (50/50 v/v) pH 7.

0.5 were obtained, which reveals that that the electrodic process is diffusion-controlled [24]. On the other hand, when the experiments were carried out in non-aqueous medium it became possible to distinguish the typical reversible monoelectronic couple corresponding to nitro radical generation ($\Delta E_p \approx 60$ mV at 10 V s^{-1}) [25].

The experimental cathodic potentials in non-aqueous medium at 1 V s^{-1} were, for NB, BNB, PMNB, PCNB, PFNB, −715, −899, −890, −870 and −850 mV, respectively, and for PNB, −936 and −1110 mV (Fig. 5B shows typical CVs for NB, PMNB and PCNB derivatives). These peak potential reduction values are in agreement with those previously described for other nitroaromatic compounds with recognized biological activity [26–31]; particularly relevant is the similarity that arises from comparing the reduction potential of the compounds tested in the present study and that of nifurtimox (−876 mV) [10,32]. Considering that the easiness of reduction of nitroaromatic compounds tends to correlate with their pharmacological activity [22,32], it seems reasonable to state that the growth and oxygen uptake inhibitory effects seen in *T. cruzi* observed previously for these 2-nitrophenylbenzimidazole [10] be attributed to their easiness to undergo nitroreduction.

3.2. Analytical applications

With analytical purposes, DPP mode was selected. In Table 2, both the optimal experimental conditions and the analytical parameters are summarized [33]. Repeatability and reproducibility at different concentration levels were adequate with RSD lower than 3%. In addition, the developed method was checked for selectivity by testing hydrolysis, photolysis, oxidation, synthesis precursor interferences and typical excipients commonly found in pharmaceutical formulations. In these experiments, no new signal or decrease of peak current in the polarograms were observed, with the exception of the hydrolysis test in which a new signal appears at more anodic potentials for BNB, PMNB, PCNB, PFNB and PNB (data not shown).

The developed polarographic methodology was applied to follow the hydrolytic degradation kinetic of BNB. Fig. 6 depicts the polarograms obtained from hydrolysis trials carried out at pH 7.4 and 25 °C. As can be seen, the polarographic peak of BNB (−485 mV) diminishes along the time of hydrolysis and a new signal appears at −333 mV, which corresponds to that of NB, the electroactive decomposition product of BNB. To test the kinetic order of the hydrolytic degradation, experiments at different initial concentrations of BNB and pH were conducted. Changes in the initial BNB concentration did not affect the slopes of the decay

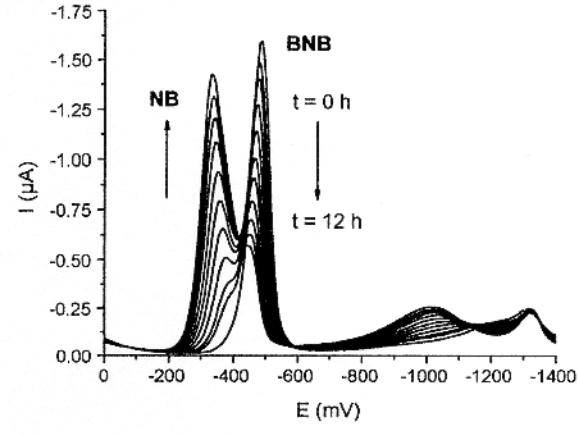

Fig. 6. DP polarograms of 1×10^{-4} mol L^{-1} BNB in ethanol/0.1 mol L^{-1} Britton–Robinson buffer (30/70 v/v) submitted to hydrolysis at pH 7.4 and 25 °C at different times.

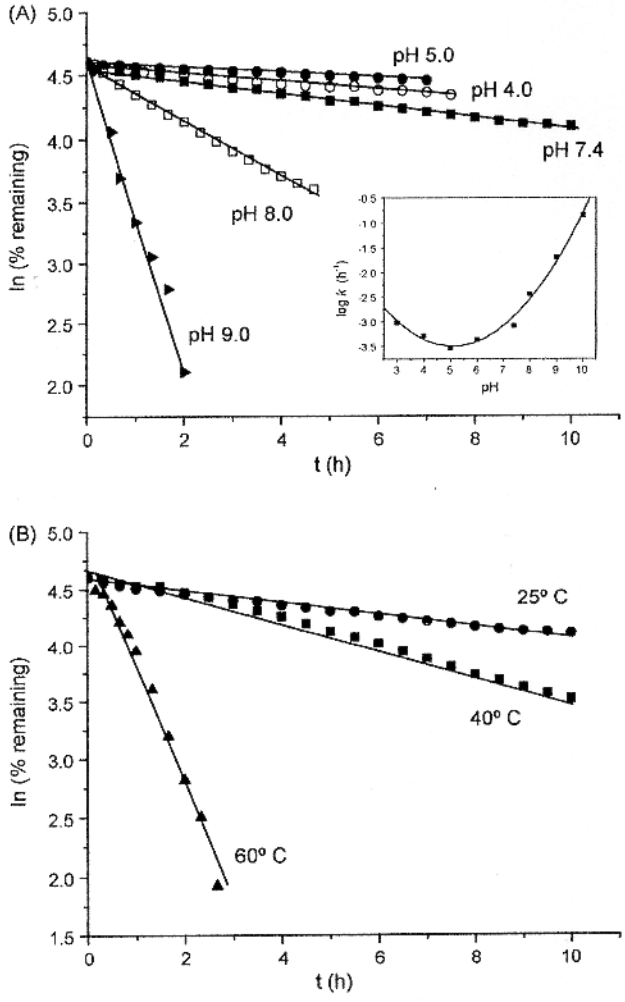

Fig. 7. (A) Effect of pH on degradation of 1.2×10^{-4} mol L^{-1} BNB solution at 25 °C, insert: pH rate profile of the hydrolysis process of BNB at 25 °C. (B) Effect of temperature on degradation of 1.2×10^{-4} mol L^{-1} BNB solution at pH 7.4.

curves, and plots of ln concentration *vs.* hydrolysis time were found to be linear (data not shown). Consequently, from these experiments we conclude that the hydrolytic degradation of BNB follows a first order kinetic [34,35].

Regarding the influence of the pH, BNB exhibited a pH-dependent degradation (Fig. 7A) and the rate constants (k) increase concomitantly with the pH. Table 3 summarizes the k values and the half-lives ($t_{1/2}$) obtained at 25 °C and different pHs. On the other hand, the hydrolysis was found to also depend on the temperature; increasing the latter, from 25 °C to 40 °C and from 40 °C to 60 °C, dramatically changed the k values by 2.3- and 20.5-fold, respectively (Fig. 7B). From Arrhenius plot, an activation energy value of 14.9 kcal/mol was calculated. This value is in agreement with that of reported for other drug undergoing hydrolytic decomposition [34]. In addition, the pH-rate profile corresponding to the hydrolysis process of BNB at 25 °C is shown in Fig. 7A (insert). As can be seen, BNB exhibits it maximum stability near its pK_a value ($pK_{a\ BNB} = 4.90$) and also presents base catalysis hydrolysis from pH 7.5 [35].

Table 3
Rate constant (k) and half-life ($t_{1/2}$) values for BNB degradation at different pHs (25 °C).

pH	k (h^{-1})	$t_{1/2}$ (h)
3.0	9.36×10^{-4}	12.3
4.0	5.17×10^{-4}	22.3
5.0	2.94×10^{-4}	39.2
6.0	4.33×10^{-4}	26.7
7.4	8.12×10^{-4}	14.2
8.0	3.58×10^{-3}	3.2
9.0	2.03×10^{-2}	0.6
10.0	1.40×10^{-1}	0.08

4. Concluding remarks

The six 2-nitrophenylbenzimidazole compounds studied in protic media by DPP, TP and CV, present two irreversible cathodic responses in a wide range of pH; a main signal was found to be due to a nitro group reduction and a second one, probably to due to the reduction of azomethine. In DPP and TP experiments, the peak potential of the main signal exhibited, for each of the tested compounds, a linear dependence with the pH, showing breaks that are in agreement with the pK_a values of each one. The differences in the reduction potentials seen amongst the derivatives were explained by both the loss of coplanarity of the nitro group from the plane to the phenyl ring and the staking between the phenyl ring of the 2-nitrophenylbenzimidazole nucleus and the N-benzoyl substituent. On the other hand, in CV experiments in non-aqueous medium was possible to distinguish the typical reversible monoelectronic couple corresponding to the nitro radical generation, and peak potential reduction values were in agreement with those previously described for other nitroaromatic compounds with recognized biological activity.

Finally, on the basis of the electrochemical response of the six new 2-nitrobenzimidazole derivatives, DPP methods were developed, exhibiting adequate accuracy, reproducibility and selectivity. These methods could be applied for the determination of these compounds in pharmaceutical forms and in further stability studies. Application of the here developed DPP methods requires no treatment of the samples, is less time-consuming and less expensive than other ones, such as HPLC or UV–vis spectrophotometry [10].

Acknowledgement

Authors are grateful for the support of FONDECYT Grant No. 1061144.

References

[1] J.D. Maya, B.K. Cassels, P. Iturriaga-Vásquez, J. Ferreira, M. Faúndez, N. Galanti, A. Ferreira, A. Morello, Comp. Biochem. Phys. A 146 (2007) 601.
[2] S.L. Croft, M.P. Barrett, J.A. Urbina, Trends Parasitol. 21 (2005) 508.
[3] Z.H. Zhang, L. Yin, Y.M. Wang, Catal. Commun. 8 (2007) 1126.
[4] J. Valdez, R. Cedillo, A. Hernández-Campos, L. Yépez, F. Hernández-Luis, G. Navarrete-Vázquez, A. Tapia, R. Cortes, M. Hernández, R. Castillo, Bioorg. Med. Chem. Lett. 12 (2002) 2221.
[5] J.H. Tocher, R.C. Knight, D.I. Edwards, Free Radic. Res. Commun. 5 (1989) 319.
[6] J.H. Tocher, Gen. Pharmacol. 28 (1997) 485.
[7] P. Kovacic, J.R. Ames, M.D. Ryan, J. Electroanal. Chem. 275 (1989) 269.
[8] J.E. Biaglow, M.E. Varnes, L. Roizen-Towle, E.P. Clark, E.R. Epp, M.B. Astor, E.J. Hall, Biochem. Pharmacol. 35 (1986) 77.
[9] B.D. Palmer, W.R. Wilson, S. Cliffe, W.A. Denny, J. Med. Chem. 35 (1992) 3214.
[10] S. Brain-Isasi, C. Quezada, H. Pessoa, A. Morello, M.J. Kogan, A. Álvarez-Lueje, Bioorg. Med. Chem. 16 (2008) 7622.
[11] J.A. Valderrama, H. Pessoa-Mahana, G. Sarrás, R. Tapia, Heterocycles 51 (1999) 2193.
[12] H. Pessoa-Mahana, C.D. Pessoa-Mahana, R. Salazar, J.A. Valderrama, E. Saez, R. Araya-Maturana, Synthesis 3 (2004) 436.
[13] H.T.S. Britton, Hydrogen Ions, 4th Ed., Chapman & Hall, London, 1952, p. 113.
[14] S. Izquierdo, M.J. Kogan, T. Parella, A.G. Moglioni, V. Branchadell, E. Giralt, R.M. Ortuño, J. Org. Chem. 69 (2004) 5093.
[15] O.A. Quattrochi, S.A. De Andrizzi, R.F. Laba, Introducción a la HPLC, Aplicación y Práctica, Artes Gráficas Farro SA, Argentina, 1992.
[16] K. Akimoto, H. Kurosaka, I. Nakagawa, K. Sugimoto, Chem. Pharm. Bull. 36 (1988) 1483.

[17] H. Lund, in: H. Lund, O. Hammerich (Eds.), Organic Electrochemistry, 4th Ed., Marcel Dekker, New York, 2001, p. 390.
[18] E. Hammam, A. Tawfik, M.M. Ghoneim, J. Pharm. Biomed. Anal. 36 (2004) 149.
[19] S.F. De Betona, J.M. Moreda, A. Arranz, J.F. Arranz, Anal. Chim. Acta 329 (1996) 25.
[20] M.M. Ghoneim, M.M. Mabrouk, A.M. Hassanein, A. Tawfik, J. Pharm. Biomed. Anal. 25 (2001) 933.
[21] A.J. Bard, L.R. Faulkner, Electrochemical Methods: Fundamentals and Applications, 2nd Ed., John Wiley & Sons, Inc., New York, 2001.
[22] L.J. Núñez-Vergara, P. Santander, P.A. Navarrete-Encina, J.A. Squella, J. Electroanal. Chem. 580 (2005) 135.
[23] A. Agostiano, P. Cosma, M. Trotta, L. Mons-Scolaro, N. Micali, J. Phys. Chem. B 106 (2002) 12820.
[24] P. Kissinger, W. Heineman, Laboratory Techniques in Electroanalytical Chemistry, 10th Ed., Marcel Dekker, New York, NY, 1984.
[25] A. Álvarez-Lueje, H. Pessoa, L.J. Núñez-Vergara, J.A. Squella, Bioelectrochem. Bioener. 46 (1998) 21.
[26] P. Kovacic, M.A. Kassel, B.A. Feinberg, M.D. Corbett, R.A. McClelland, Bioorg. Chem. 18 (1990) 265.
[27] P. Wardman, Environ. Health Persp. 64 (1985) 309.
[28] C. Viodé, N. Bettache, N. Cenas, R.L. Krauth-Siegel, G. Chauvière, N. Bakalara, J. Périé, Biochem. Pharmacol. 57 (1999) 549.
[29] J. Argüello Da Silva, L.J. Núñez Vergara, S. Bollo, J.A. Squella, J. Electroanal. Chem. 591 (2006) 99.
[30] F.C. de Abreu, P.A.L. Ferraz, M.O.F. Goulart, J. Braz. Chem. Soc. 13 (2002) 19.
[31] F. Santos de Paula, E.M. Sales, M. Vallaro, R. Fruttero, M.O.F. Goulart, J. Electroanal. Chem. 579 (2005) 33.
[32] S. Bollo, L.J. Núñez-Vergara, M. Bonta, G. Chauviere, J. Perie, J.A. Squella, J. Electroanal. Chem. 511 (2001) 46.
[33] J. Ermer, J.H.McB. Miller (Eds.), Method Validation in Pharmaceutical Analysis. A Guide to Best Practice, Wiley-VCH Verlag GmbH & Co., KGaA, Weinheim, 2005.
[34] K.A. Connors, C.L. Amidon, V.J. Stella, Chemical Stability of Pharmaceuticals: A Handbook for Pharmacist, J. Willey, New York, 1986.
[35] S. Yoshioka, V.J. Stella, Stability of Drugs and Dosage Forms, Kluwer Academic Publishers, New York, 2002.